Redox Biology 24 (2019) 101180

Contents lists available at ScienceDirect

Redox Biology

journal homepage: www.elsevier.com/locate/redox

Cholesterol crystals promote endothelial cell and monocyte interactions via H_2O_2-mediated PP2A inhibition, NFκB activation and ICAM1 and VCAM1 expression

Prahalathan Pichavaram, Arul M. Mani, Nikhlesh K. Singh, Gadiparthi N. Rao*

Department of Physiology, University of Tennessee Health Science Center, Memphis, TN 38163, USA

ARTICLE INFO

Keywords:
Cholesterol crystals
H_2O_2
PP2A
NFκB
ICAM1/VCAM1
Xanthine oxidase
EC-Monocyte interactions

ABSTRACT

In the present study, we show that cholesterol crystals induce NFκB activation, and ICAM1 and VCAM1 expression via xanthine oxidase-mediated H_2O_2 production and PP2A inhibition in influencing endothelial cell and monocyte interactions and all these adverse effects of cholesterol crystals could be attenuated by proresolving lipid mediator RvD1. In addition, feeding mice with cholesterol rich diet (CRD) increased xanthine oxidase expression, its activity and H_2O_2 production leading to PP2A inhibition, NFκB activation, and ICAM1 and VCAM1 expression and RvD1 attenuated all these effects of CRD substantially. Furthermore, peripheral blood mononuclear cells (PBMCs) from wild type mice when injected into mice that were fed with CRD or RvD1 + CRD showed increased leukocyte trafficking to arteries of CRD-fed mice as compared to RvD1 + CRD mice. These findings suggest that cholesterol crystals via promoting oxidant stress and inhibiting Ser/Thr phosphatases such as PP2A stimulate NFκB activation and ICAM1 and VCAM1 expression, and thereby enhance EC-monocyte interactions. In addition, proresolving lipid mediators such as RvD1 appear to exert their anti-inflammatory effects via countering the adverse effects of cholesterol crystals or CRD.

1. Introduction

Endothelium, the single innermost cell layer of the vascular wall, plays a key role in vascular function by regulating vascular tone, inhibiting platelet and leukocyte adhesion and limiting vascular proliferation [1]. Dysfunctional endothelium, as characterized by increased permeability, enhanced stickiness to platelets and leukocytes and heightened production of cytokines, provokes the pathogenesis of various vascular diseases including atherosclerosis and hypertension [2,3]. The expression of adhesion molecules such as ICAM1 and VCAM1 by the dysfunctional endothelium triggers the adherence of leukocytes to the endothelium and their subsequent transmigration into the vessel wall, an important event in setting vascular inflammation [4,5]. These events appear to be mediated by increased ROS production and NFκB activation [6,7]. A large amount of evidence also shows that dysfunctional endothelium generates excessive ROS production [8,9].

RvD1, a specialized proresolving lipid mediator, exhibits anti-inflammatory effects both in vitro and in vivo [10]. In addition, it has been reported that RvD1 protects endothelial adherens junction integrity and barrier function [11]. In recent years, many studies have reported the presence of cholesterol crystals in human atherosclerotic plaques [12–14]. It was also reported that cholesterol crystals promote plaque vulnerability and rupture [14,15]. Besides, studies from our laboratory showed that cholesterol crystals induce foam cell formation [16], disrupt adherens junctions and increase vascular permeability [17]. Based on these observations, we wanted to test whether cholesterol crystals have any effect on endothelial cell (EC)-monocyte interactions, and if so, the efficacy of RvD1 in suppressing these effects. Here, we show that cholesterol crystals via xanthine oxidase-mediated H_2O_2 production, PP2A inactivation, NFκB activation and ICAM1 and VCAM1 expression trigger EC-monocyte interactions. In addition, our findings reveal that RvD1 prevents cholesterol crystals-induced EC-monocyte interactions via suppressing H_2O_2-mediated PP2A inhibition, NFκB activation and ICAM1 and VCAM1 expression. Furthermore, mice fed with CRD showed increased expression and activity of XO, H_2O_2 production, PP2A inhibition, NFκB activation and ICAM1 and VCAM1

Abbreviations: CC, cholesterol crystals; CD, chow diet; CRD, cholesterol-rich diet; HAECs, human aortic endothelial cells; H_2O_2, hydrogen peroxide; ICAM1, inter cellular adhesion molecule 1; NFκB, nuclear factor kappa B; PP2A, protein phosphatase 2A; RvD1, Resolvin D1; VCAM1, vascular cell adhesion molecule 1; WT, wild type; XO, xanthine oxidase

* Corresponding author. Department of Physiology, University of Tennessee Health Science Center, 71 S. Manassas Street, Memphis, TN 38163, USA.
E-mail address: rgadipar@uthsc.edu (G.N. Rao).

https://doi.org/10.1016/j.redox.2019.101180
Received 12 March 2019; Accepted 26 March 2019
Available online 03 April 2019

expression in their arteries with enhanced stickiness to leukocytes and RvD1 attenuates all these adverse effects of CRD.

2. Materials and methods

Reagents: Anti-ICAM1 (SC-18853), anti-VCAM1 (SC-13160), anti-IKKα/β (SC-7607), anti-IκBα (SC-1643), anti-NFκB (SC-3721), anti-pPP2A-C(α/β) (SC-12615R), anti-PP2A-C(α/β) (SC-56950), anti-α-tubulin (SC-23948) and anti-XO (SC-398548) antibodies were purchased from Santa Cruz Biotechnology (Santa Cruz, CA). Neutralizing anti-ICAM1 (ab171123), pIKKα/β (ab194528) and neutralizing anti-VCAM1 (ab47159) antibodies were obtained from Abcam (Cambridge, MA). Cytostatin (19602), pyrrolidinedithiocarbamic acid (PDTC) (20713), QNZ (10006734) and Resolvin D1 (10012554) were purchased from Cayman Chemical Company, (Ann Arbor, MI). Anti-pIκBα (2859) and anti-pNFκB (3033) antibodies were obtained from Cell Signaling Technology (Beverly, MA). Ser/Thr phosphatase assay kit (17127) was bought from Millipore (Temecula, CA). Amplex Red Hydrogen Peroxide Assay kit (A22188), Pierce LAL Chromogenic Endotoxin Quantification kit (88282), Medium 200 (M200500), Low Serum Growth Supplements (S003K), BCECF (B1170) and gentamycin/amphotericin solution (R01510) were obtained from ThermoFisher Scientific (Waltham, MA). Allopurinol (PHR1377) and PKH67 Green Fluorescent Cell Linker kit (PKH67GL) were bought from Sigma Aldrich Company (St Louis, MO).

Cell culture: Human aortic endothelial cells (HAECs) (Cat. No. H6052) were purchased from Cell Biologics (Chicago, IL) and cultured in Medium 200 containing low serum growth supplements (LSGS), 10 μg/ml gentamycin and 0.25 μg/ml amphotericin B. Cultures were maintained at 37 °C in a humidified 95% air and 5% CO_2 atmosphere. HAECs between 6 and 10 passages were growth-arrested by incubating in Medium 200 without LSGS for 6 h and used to perform the experiments unless otherwise indicated.

Animals: C57BL/6 mice were purchased from Charles River Laboratories (Wilmington, MA). Mice were maintained at UTHSC vivarium according to the Institutional Animal Care and Use Committee's guidelines. The Animal Care and Use Committee of the University of Tennessee Health Science Center, Memphis, TN, approved all the experiments involving animals. Mice were fed with cholesterol rich diet (Cat. No. D12108C, Research Diets, New Brunswick, NJ) in combination with and without RvD1 (10 μg/kg body weight every 2 days) or left on CD for 12 weeks and used. At the end of the experimental period, mice were sacrificed by ketamine/xylazine overdose and the aortas were isolated for further analysis as required.

Preparation of cholesterol crystals: Cholesterol crystals were prepared as described previously [16]. Briefly, 25 g of anhydrous cholesterol was dissolved in 2 L of prewarmed (60 °C) 95% ethanol. While warm, the mixture was filtered through a Whatman 1 paper to remove the particles. The filtrate was then left at room temperature overnight and the sedimented cholesterol crystals were collected by filtration through Whatman 1 paper and dried at room temperature. The same procedure was repeated twice in order to obtain pure monohydrated cholesterol crystals. The crystals were grounded using a mortar and pestle and stored in an amber colored bottle at −20 °C and used as needed.

H_2O_2 production assay: HAECs with and without the indicated treatments were collected by scraping into PBS and 50 μl of the cell suspension was incubated with 50 μl of 100 μM Amplex Red along with 0.2 U/ml of HRP for 30 min at 37 °C in the dark. Following incubation, the fluorescence intensity was measured in SpectraMax Gemini XPS Spectrofluorometer (Molecular Devices) with excitation at 530 nm and emission at 590 nm. The H_2O_2 production was expressed as RFU.

Immunoprecipitation: Immunoprecipitation was performed as described previously [18]. Cell or tissue extracts containing equal amount of protein from control and the indicated treatments was incubated with the indicated primary antibody at 1:100 dilution overnight at 4 °C. Protein A/G-conjugated Sepharose CL-4B beads (50 μl of 50% slurry) were added and incubation continued for an additional 1 h at room temperature and the beads were collected by centrifugation at 1000 rpm for 1 min at 4 °C. The beads were washed three times with lysis buffer (PBS, 1% Nonidet P40, 0.5% sodium deoxycholate, 0.1% SDS, 100 μg/ml PMSF, 100 μg/ml aprotinin, 1 μg/ml leupeptin, 1 M glycerophosphate and 1 mM sodium orthovanadate) and once with PBS, boiled in SDS sample buffer and analyzed by immunoblotting.

Western blot analysis: Cell or tissue extracts containing equal amounts of protein from control and the indicated treatments were resolved by SDS-PAGE. The proteins were transferred electrophoretically to a nitrocellulose membrane. After blocking in either 5% (W/V) nonfat dry milk or 5% (W/V) BSA, the membrane was probed with appropriate primary antibodies followed by incubation with horseradish peroxidase-conjugated secondary antibodies. The antigen-antibody complexes were detected using enhanced chemiluminescence detection reagents.

PP2A activity: To measure PP2A activity, the cell or tissue extracts containing equal amounts of protein were immunoprecipitated with anti-PP2A antibody and the immunocomplexes were analyzed for phosphatase activity as described by Narayanan et al. [19].

Monocyte adhesion: THP1 cell adhesion to HAEC monolayer was measured using a fluorometric method [18]. HAEC monolayer was grown to confluency, quiesced and treated with and without cholesterol crystals (200 μg/ml) for 2 h. Wherever RvD1, pharmacological inhibitors or neutralizing antibodies were used, they were added to cells 30 min prior to treatment with and without cholesterol crystals. THP1 cells that were labeled with 10 μM BCECF in serum-free medium for 30 min were placed on HAEC monolayer at 8×10^4 cells/well, and incubation continued for another 1 h. After incubation, the non-adherent cells were washed off with PBS and the adherent cells were lysed in 0.2 ml of 0.1 M Tris-HCl buffer, pH 8.0, containing 0.1% Triton X-100. The fluorescence intensity was measured in a Spectra Max Gemini XPS Spectroflurometer (Molecular Device) with excitation at 485 nm and emission at 535 nm. Cell adhesion was expressed as RFU.

Monocyte transmigration: THP1 cell transmigration through HAEC monolayer was measured as described previously [20]. HAECs that were grown to confluency and quiesced for 6 h in serum-free Medium 200 were treated with and without cholesterol crystals for 2 h. Wherever RvD1, pharmacological inhibitors or neutralizing antibodies were used, they were added to HAEC monolayer 30 min prior to treatment with and without cholesterol crystals. Then, THP1 cells labeled with BCECF were added at 1×10^5 cells/well onto HAEC monolayer and incubation continued overnight at 37 °C. After incubation, medium was removed, cells were washed with PBS and culture inserts were removed. Cells on top of the inserts were removed with cotton swab, fixed with methanol for 10 min and placed on slides upside down. Cells were observed under a Zeiss fluorescence microscope (Axio Observer.Z1) using a 10X/NA 0.6 objective and the images were captured by AxioCam MRm camera without any enhancements using the microscope operating and image analysis software Axiovision Version 4.7.2 (Carl Zeiss Imaging Solutions GmbH).

Isolation of peripheral blood mononuclear cells (PBMCs): Mice were anesthetized with ketamine/xylazine. Blood was collected by cardiac puncture into BD Vacutainer K2 EDTA tubes and diluted with an equal volume of PBS. Blood was then overlaid on the top of Lymphoprep solution (2:1) and centrifuged at 1500 rpm for 30 min at 4 °C. The white buffy coat layer enriched with PBMCs was collected, washed with PBS, resuspended in PBS, and labeled with PKH67 green fluorescent cell tracker according to the manufacturer's instructions.

In vivo leukocyte adhesion assay: WT mice fed with CRD alone or in combination with RvD1 or left on CD for 3 months were anesthetized with ketamine/xylazine, and peripheral blood mononuclear cells isolated from WT mice were injected via tail vein (1×10^6 cells/mice). Twenty-four hours later, aortas were isolated, cleaned, fixed, opened, stained with DAPI, mounted on a slide with luminal side up and examined under a Zeiss inverted microscope (Axio Observer.Z1, 40X/NA

0.16). The fluorescence images were captured with a Zeiss AxioCam MRm camera using the microscope operating and image analysis software AxioVision version 4.7.2 (Carl Zeiss Imaging Solutions GmbH), and PKH67-positive cells were counted.

Statistics: All the experiments were performed three times and the data were presented as Mean ± SD. The treatment effects were analyzed by one-way ANOVA followed by Tukey's post hoc test or Student's *t*-test using GraphPad Prism software (5.03) and the p values < 0.05 were considered to be statistically significant.

3. Results

3.1. Cholesterol crystals induce ICAM1 and VCAM1 expression in endothelial cells via activation of NFκB

Many studies have demonstrated the presence of cholesterol crystals in atherosclerotic plaques and their role in inflammasome formation [13–15,21]. But the underlying mechanisms of inflammation and atherosclerotic lesion progression by cholesterol crystals were not fully understood. As endothelial dysfunction [3,6] and inflammation [2] are linked to the development of atherosclerosis and to understand the potential mechanisms by which cholesterol crystals influence these events, we tested the effect of cholesterol crystals on the expression of cell adhesion molecules. Cholesterol crystals increased both ICAM1 and VCAM1 expression in a time dependent manner (Fig. 1A). Since adhesion molecules play a critical role in the recruitment of monocytes to and transmigration through the EC monolayer into the artery and thereby influence inflammation [4,22,23], we tested the effect of cholesterol crystals on HAEC and monocyte interactions. Cholesterol crystals induced monocyte adhesion to HAECs and neutralizing anti-ICAM1 or anti-VCAM1 antibodies substantially inhibited this effect (Fig. 1B). Similarly, cholesterol crystals induced transmigration of monocytes through HAEC monolayer and this effect was also suppressed by both anti-ICAM1 and anti-VCAM1 neutralizing antibodies (Fig. 1C). The observed effects of cholesterol crystals on cell adhesion molecules expression and EC-monocyte interactions were not due to their contamination with LPS as cholesterol crystals were found to be free of endotoxin (Fig. 1D). A large body of evidence shows that NFκB mediates ICAM1 and VCAM1 expression in response to many agonists [5,24,25]. To understand the mechanisms by which cholesterol crystals induce ICAM1 and VCAM1 expression in HAECs, we tested the role of NFκB. Cholesterol crystals induced IKKα/β, IκBα and NFκB phosphorylation in a time dependent manner (Fig. 2A). In addition, pharmacological inhibitors of NFκB, namely PDTC and QNZ [26], blocked cholesterol crystals-induced IKKα/β, IκBα and NFκB phosphorylation and ICAM1 and VCAM1 expression (Fig. 2B). Inhibition of NFκB also blocked cholesterol crystals-induced adhesion of monocytes to HAECs and their transmigration through HAEC monolayer (Fig. 2C and D).

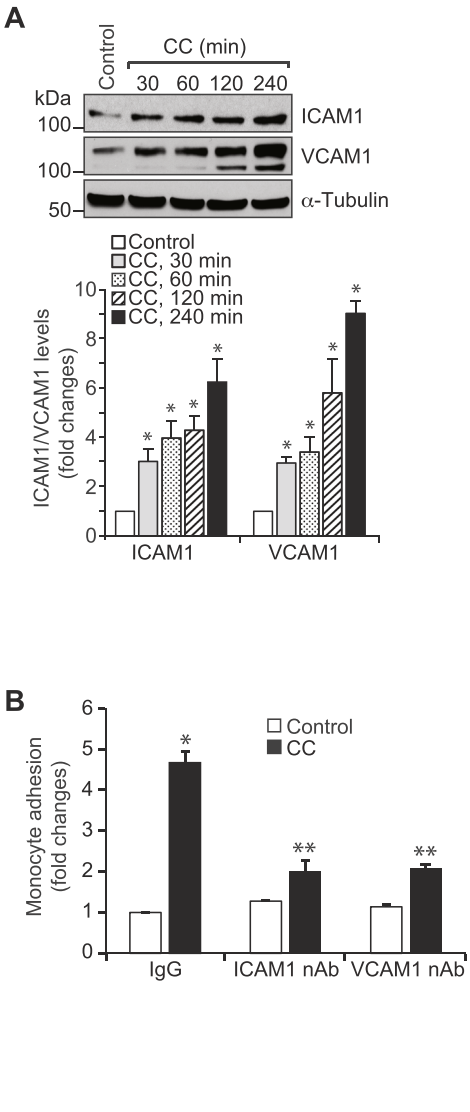

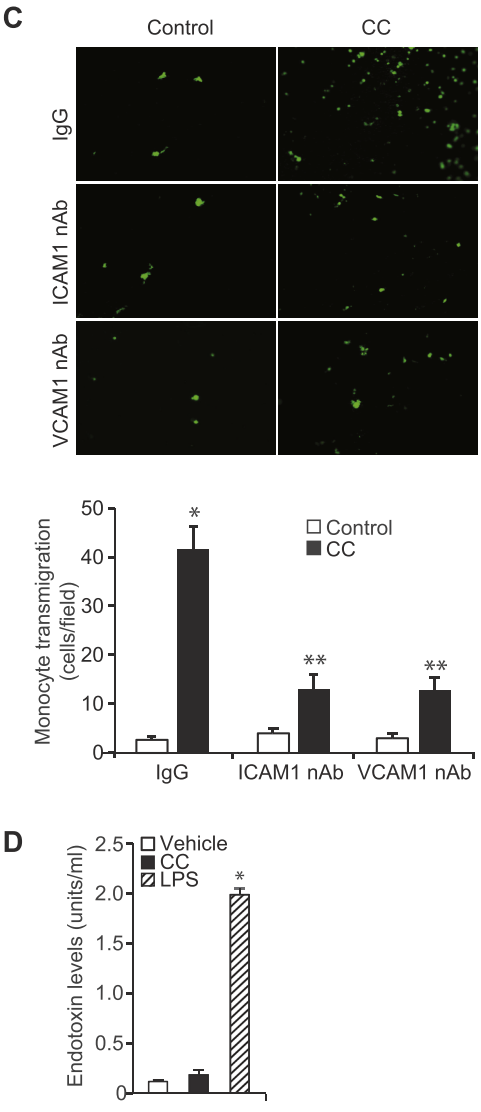

Fig. 1. CCs stimulate endothelial cell and monocyte interactions via ICAM1 and VCAM1 expression. A. An equal amount of protein from control and the indicated time periods of CCs (200 μg/ml)-treated HAECs were analyzed by Western blotting for ICAM1 and VCAM1 expression using their specific antibodies and the blot was normalized for α-tubulin. B & C. Quiescent HAEC monolayer was treated with and without CCs (200 μg/ml) in the presence and absence of neutralizing anti-ICAM1 or anti-VCAM1 antibodies (2 μg/dish) for 2 h and subjected to THP1 cell adhesion (B) and transmigration (C) assays. D. CCs were tested for endotoxin using Pierce LAL Chromogenic Endotoxin Quantification kit following the supplier's instructions. The bar graphs represent quantitative analysis of three experiments. The values are expressed as Mean ± SD. *p < 0.05 vs control or IgG; **p < 0.05 vs IgG + CCs.

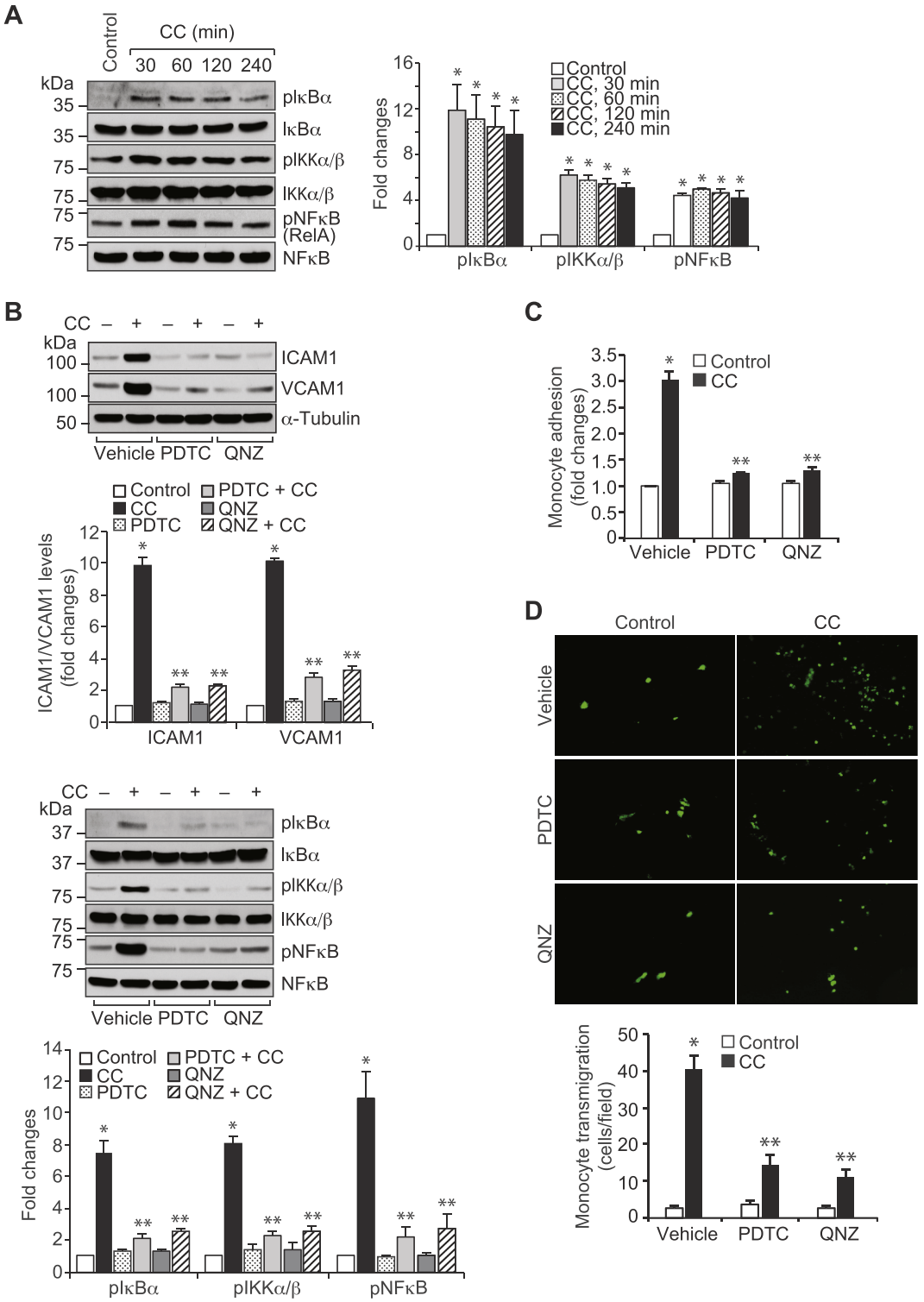

Fig. 2. CCs-induced ICAM1 and VCAM1 expression and EC-monocyte interactions require NFκB activation. A. An equal amount of protein from control and the indicated time periods of CCs (200 μg/ml)-treated HAECs were analyzed by Western blotting for pIκBα, pIKKα/β and pNFκB using their phospho-specific antibodies and the blots were normalized to their total levels. B. Quiescent HAECs were treated with and without CCs (200 μg/ml) in the presence and absence of PDTC (50 μM) or QNZ (10 μM) for 1 h or 30 min and cell extracts were prepared and analyzed by Western blotting for the indicated proteins (1 h samples for ICAM1 and VCAM1 expression and 30 min samples for pIκBα, pIKKα/β and pNFκB levels) using their specific antibodies and the blots were normalized for α-tubulin or their respective total levels. C & D. Quiescent HAEC monolayer was treated with and without CCs (200 μg/ml) in the presence and absence of PDTC (50 μM) or QNZ (10 μM) for 2 h and subjected to THP1 cell adhesion (C) and transmigration (D) assays. The bar graphs represent quantitative analysis of three experiments. The values are expressed as Mean ± SD. *p < 0.05 vs control; **p < 0.05 vs vehicle + CCs.

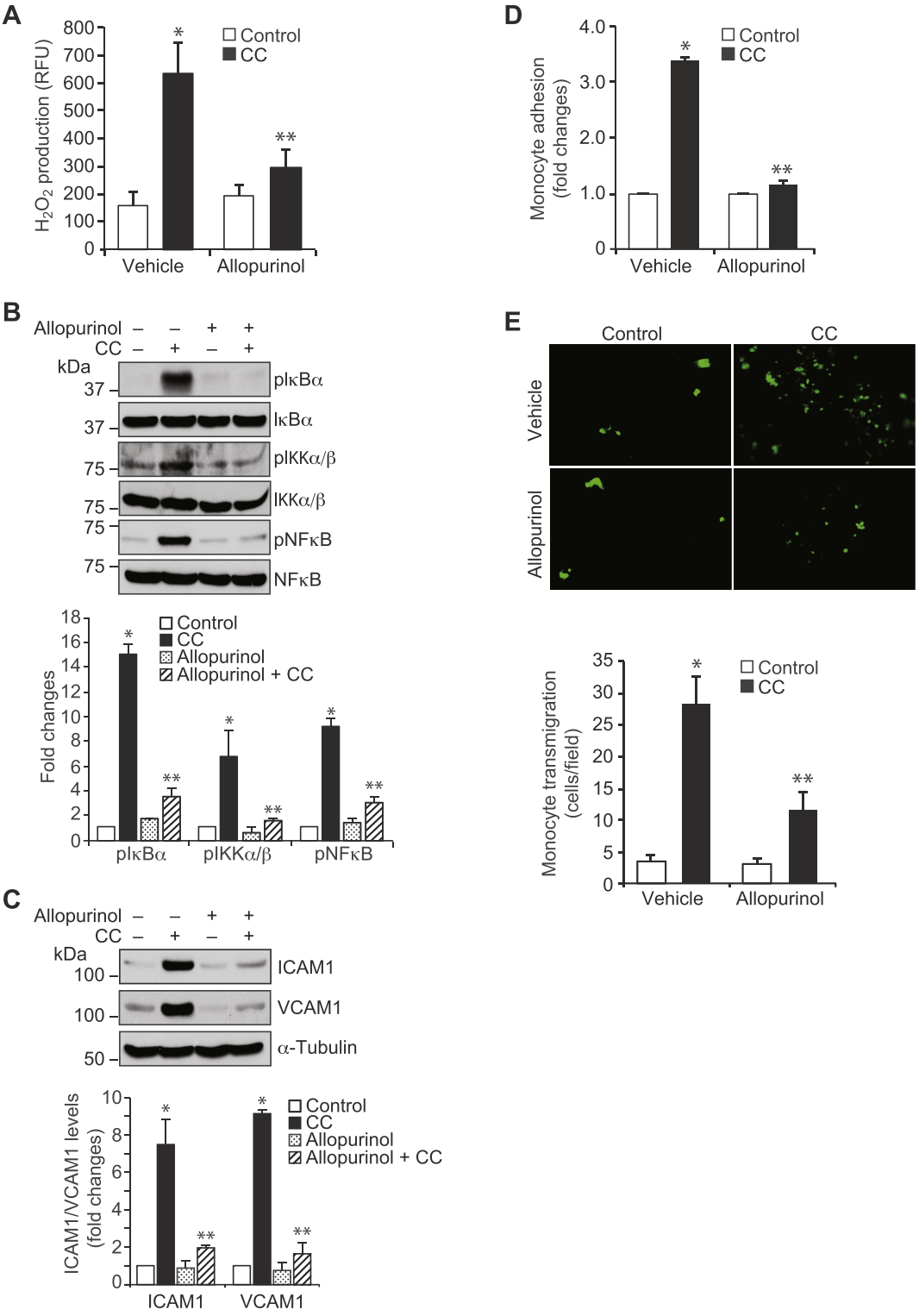

Fig. 3. XO-mediated H_2O_2 production is required for CCs-induced NFκB activation, ICAM1 and VCAM1 expression and EC-monocyte interactions. A. Quiescent HAECs were treated with and without CCs (200 μg/ml) in the presence and absence of Allopurinol (50 μM) for 10 min and assayed for H_2O_2 production. B & C. Quiescent HAECs were treated with and without CCs (200 μg/ml) in the presence and absence of Allopurinol (50 μM) for 30 min (B) or 1 h (C) and cell extracts were prepared and analyzed by Western blotting for the indicated proteins using their specific antibodies. D & E. Quiescent HAEC monolayer was treated with and without CCs (200 μg/ml) in the presence and absence of Allopurinol (50 μM) for 2 h and subjected to THP1 cell adhesion (D) and transmigration (E) assays. The bar graphs represent quantitative analysis of three experiments. The values are expressed as Mean ± SD. *p < 0.05 vs control; **p < 0.05 vs CCs or vehicle + CCs.

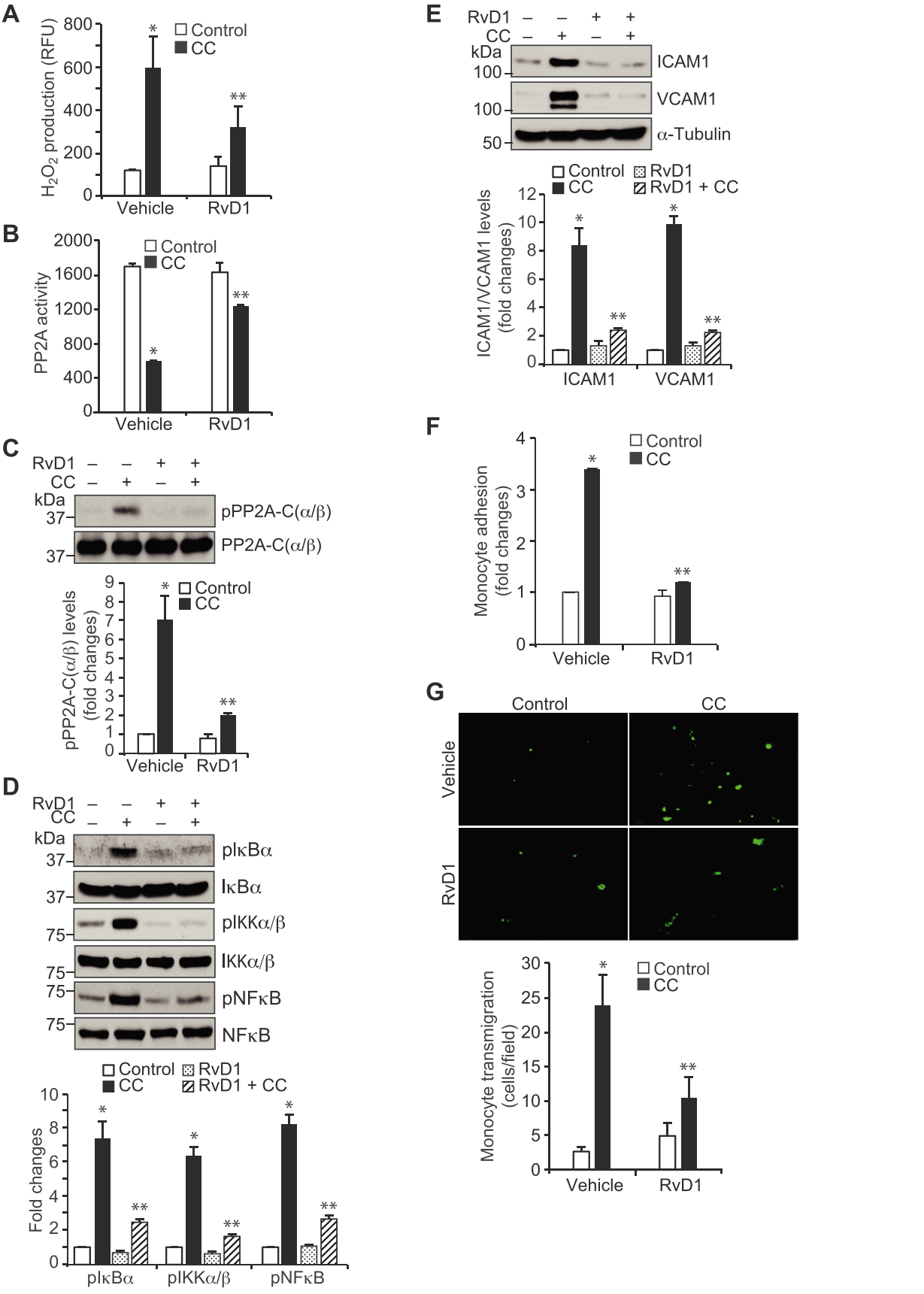

(caption on next page)

Fig. 4. RvD1 attenuates CCs-induced NFκB activation, ICAM1 and VCAM1 expression and EC-monocyte interactions by protecting PP2A from H_2O_2-mediated inhibition. A & B. Quiescent HAECs were treated with and without CCs (200 μg/ml) in the presence and absence of RvD1 (200 ng/ml) for 10 min or 30 min and assayed for H_2O_2 production (A) or PP2A activity (B), respectively. C-E. Quiescent HAECs were treated with and without CCs (200 μg/ml) in the presence and absence of RvD1 (200 ng/ml) for 30 min or 1 h and cell extracts were prepared and analyzed by Western blotting for pPP2A-C(α/β), pIκBα, pIKKα/β and pNFκB levels (30 min samples) and ICAM1 and VCAM1 expression (1 h samples) and the blots were normalized for their total levels or α-tubulin. F & G. Quiescent HAEC monolayer was treated with and without CCs (200 μg/ml) in the presence and absence of RvD1 (200 ng/ml) for 2 h and subjected to THP1 cell adhesion (F) and transmigration (G) assays. The bar graphs represent quantitative analysis of three experiments. The values are expressed as Mean ± SD. *$p < 0.05$ vs control; **$p < 0.05$ vs CCs or vehicle + CCs.

3.2. Xanthine oxidase-dependent H_2O_2 production mediates cholesterol crystals-induced NFκB activation and ICAM1 and VCAM1 expression in endothelial cells

Previously, we have shown that cholesterol crystals trigger H_2O_2 production via xanthine oxidase activation [27]. Based on these findings, we tested the role of xanthine oxidase-mediated H_2O_2 production in cholesterol crystals-induced NFκB activation. As expected, cholesterol crystals induced H_2O_2 production and Allopurinol, a specific inhibitor of xanthine oxidase [28], suppressed this effect (Fig. 3A). Allopurinol also inhibited cholesterol crystals-induced IKKα/β, IκBα and NFκB phosphorylation and ICAM1 and VCAM1 expression (Fig. 3B and C). Consistent with these observations, inhibition of xanthine oxidase by Allopurinol also blocked cholesterol crystals-induced adhesion of monocytes to HAECs and their transmigration through HAEC monolayer (Fig. 3D and E).

3.3. Resolvin D1 blocks NFκB activation and ICAM1 and VCAM1 expression by protecting PP2A activity from oxidant-mediated inhibition

Resolvins, a group of specialized proresolving lipid mediators produced by metabolic conversion of omega 3 polyunsaturated fatty acids, particularly docosahexaenoic acid and eicosapentaenoic acid have been shown to possess anti-inflammatory functions [10]. Since cholesterol crystals induced NFκB activation and ICAM1 and VCAM1 expression, which are implicated in the propagation of inflammation [21–23], we asked the question whether Resolvin D1 counters these effects. RvD1 attenuated cholesterol crystals-induced H_2O_2 production and protected PP2A activity from inhibition (Fig. 4A and B). RvD1 also blocked cholesterol crystals-induced PP2A-C(α/β) tyrosine phosphorylation (Fig. 4C). In line with these observations, RvD1 suppressed IKKα/β, IκBα and NFκB phosphorylation and ICAM1 and VCAM1 expression (Fig. 4D and E). RvD1 also inhibited cholesterol crystals-induced adhesion of monocytes to HAECs and their transmigration through HAEC monolayer (Fig. 4F and G). If the anti-inflammatory effects of RvD1 were due to its protection of PP2A from oxidant-mediated inhibition, then one would expect that pharmacological inhibition of PP2A should negate its effects. Indeed, in the presence of cytostatin, a specific inhibitor PP2A [29], RvD1 failed to block cholesterol crystals-induced IKKα/β, IκBα and NFκB phosphorylation and ICAM1 and VCAM1 expression (Fig. 5A and B). Consistent with these observations, inhibition of PP2A by cytostatin completely negated the effect of RvD1 in blocking cholesterol crystals-induced adhesion of monocytes to HAECs and their transmigration through HAEC monolayer (Fig. 5C and D).

3.4. CRD triggers xanthine oxidase-dependent H_2O_2 production, PP2A inactivation, NFκB activation and ICAM1/VCAM1 expression and RvD1 negates these effects

To validate the in vitro observations in vivo, WT mice were fed with CRD in the presence and absence of RvD1 (10 μg/kg body weight by IP every 3rd day) or left on CD for 12 weeks and tested for XO expression and its activity, PP2A activity, NFκB activation and ICAM1 and VCAM1 expression. Feeding mice with CRD for 12 weeks led to increased expression and activity of XO that in turn augmented H_2O_2 production (Fig. 6A–C). CRD feeding also led to increased PP2A-C(α/β) tyrosine phosphorylation and its inhibition (Fig. 6D and E). In addition, feeding mice with CRD induced IKKα/β, IκBα and NFκB phosphorylation and ICAM1 and VCAM1 expression (Fig. 6F and G). RvD1 inhibited all these adverse effects of CRD on XO expression and its activity, H_2O_2 production, PP2A-C(α/β) tyrosine phosphorylation and its inactivation, NFκB activation and ICAM1 and VCAM1 expression (Fig. 6A–G). To find whether CRD feeding activates endothelium rendering it more susceptible to leukocyte stickiness and RvD1 aborgates this effect, PBMCs were isolated from WT donor mice and injected into mice that were fed with CRD or RvD1 + CRD or left on CD for 12 weeks and 24 h later the aortas were isolated and examined for the adhesion of leukocytes. As compared with aortas from CD-fed mice, the aortas from CRD-fed mice showed increased adhesion of leukocytes (Fig. 7A and B). The aortas from RvD1 + CRD-fed mice showed substantially lower number of adhered leukocytes as compared to aortas from CRD-fed mice (Fig. 7A and B).

4. Discussion

Vascular endothelium is a primary site of immunological attack in inflammatory vascular diseases, and its dysfunction can lead to the development of atherosclerosis [30–32]. In the initial stages of atherogenesis, endothelial cell expression of adhesion molecules such as ICAM1 and VCAM1 enhances leukocyte recruitment to the endothelium and sets the soil for the initiation of vascular inflammation [33,34]. Several studies have shown the presence of cholesterol crystals in the atherosclerotic plaques and considered to be involved in provoking local inflammation [13–15]. In fact, it was reported that cholesterol crystals induce inflammasome formation and generate proinflammatory cytokines [21]. Previously, we have reported that cholesterol crystals induce foam cell formation [16], whose accumulation in the artery leads to lesion progression [35]. We have also reported that cholesterol crystals disrupt endothelial cell adherens junctions and increase its barrier permeability [17]. In fact, a recent study also showed that endothelial cells when overloaded with intracellular cholesterol levels in conditions such as hyperlipidemia triggers cholesterol crystal production, that in turn disrupts endothelial cell barrier function [36]. Cholesterol crystal production was also reported in hepatocytes when mice were fed with increased dietary cholesterol [37]. In the present study, we show that cholesterol crystals besides their effect on adherens junction disruption induce ICAM1 and VCAM1 expression in endothelial cells, which could support its role in inflammation. A large number of studies have shown that NFκB plays a role in the expression of cell adhesion molecules in response to inflammatory cytokines [5,24,25]. In line with these findings, we found that cholesterol crystals activate NFκB in mediating the expression of ICAM1 and VCAM1 in endothelial cells. The presence of activated NFκB in human and experimental atherosclerotic lesions has also been reported [38,39].

A large number of studies have shown that ROS mediate NFκB activation [40,41]. A role for ROS in the expression of cell adhesion molecules has also been reported [42,43]. In exploring the mechanisms by which cholesterol crystals activate NFκB, we found that cholesterol crystals induce H_2O_2 production by increasing XO activity. Indeed, XO-mediated H_2O_2 production appears to be required for cholesterol crystals-induced NFκB activation and ICAM1 and VCAM1 expression and EC-monocyte interactions, as all these effects were suppressed by

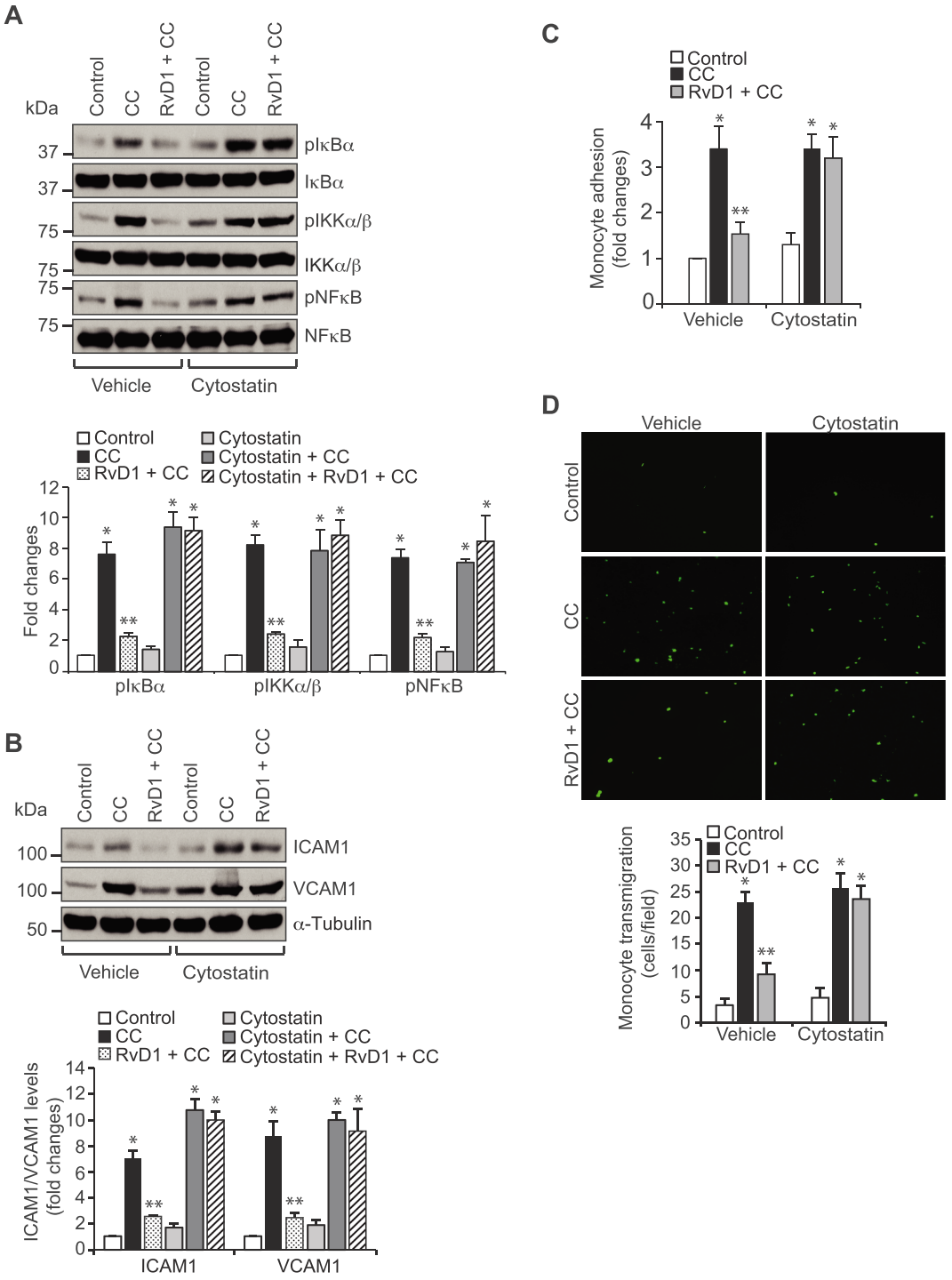

Fig. 5. Pharmacological inhibition of PP2A blocks the efficacy of RVD1 to suppress CCs-induced NFκB activation, ICAM1 and VCAM1 expression and EC-monocyte interactions. A & B. Quiescent HAECs were treated with and without CCs (200 μg/ml) in the presence and absence of RvD1 (200 ng/ml) alone or in combination with and without cytostatin (10 μM) for 30 min or 1 h and cell extracts were prepared and analyzed by Western blotting for pIκBα, pIKKα/β and pNFκB levels (30 min samples) or ICAM1 and VCAM1 expression (1 h samples) and the blots were normalized to their total levels or α-tubulin. C & D. Quiescent HAEC monolayer was treated with and without CCs (200 μg/ml) in the presence and absence of RvD1 (200 ng/ml) alone or in combination with and without cytostatin (10 μM) for 2 h and subjected to THP1 cell adhesion (C) and transmigration (D) assays. The bar graphs represent quantitative analysis of three experiments. The values are expressed as Mean ± SD. *p < 0.05 vs control; **p < 0.05 vs CCs or vehicle + CCs.

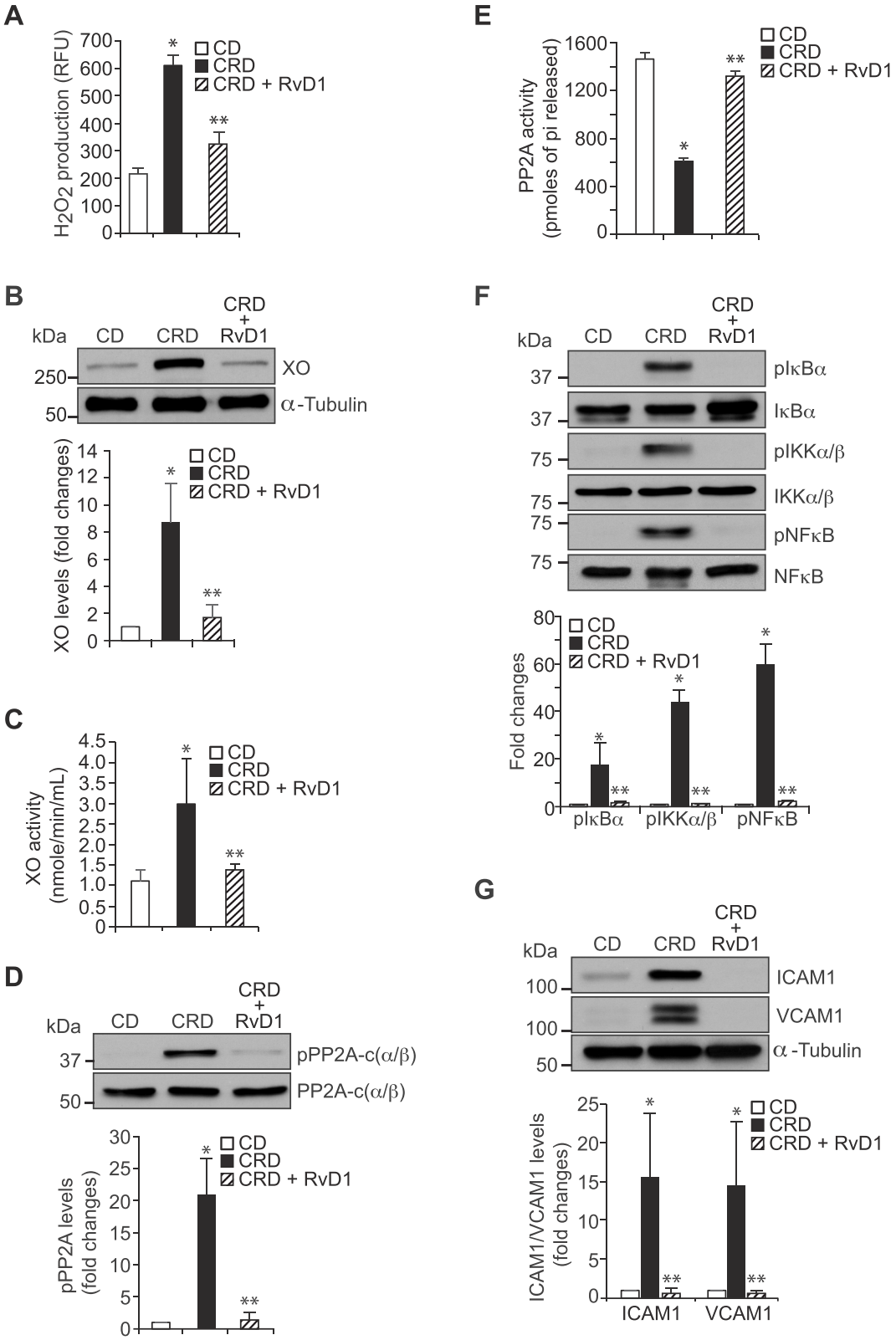

Fig. 6. RvD1 inhibits CRD-induced XO expression and its activity, PP2A inactivation, NFκB activation and ICAM1 and VCAM1 expression. A, C & E. Eight weeks old C57BL/6 mice were fed with CRD in combination with and without RvD1 (10 μg/kg body weight, every 3 days by IP) or left on CD for 12 weeks, aortas were isolated and either tissue extracts were prepared and assayed for H_2O_2 production (A) or XO and PP2A activities (C & E). B, D, F & G. An equal amount of protein from aortic tissue extracts prepared as in panel A were analyzed by Western blotting for XO, pPP2A-C(α/β), pIκBα, pIKKα/β and pNFκB, ICAM1 and VCAM1 levels and the blots were normalized for α-tubulin or their total levels. The bar graphs represent quantitative analysis of three experiments. The values are expressed as Mean ± SD. *p < 0.05 vs CD; **p < 0.05 vs CRD.

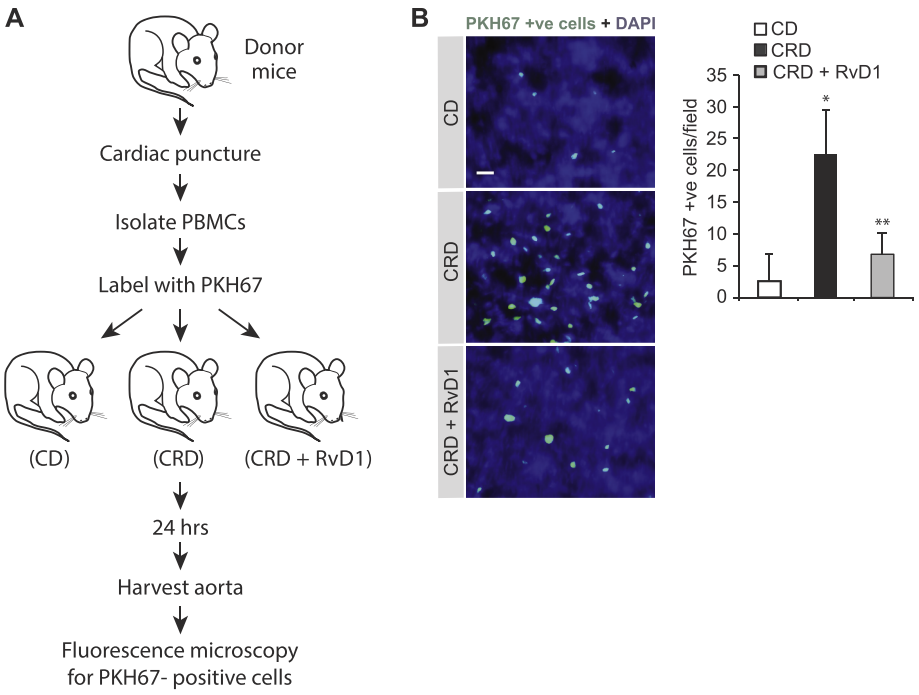

Fig. 7. RvD1 protects CRD-triggered leukocyte adhesion to arteries. PBMCs were isolated from WT donor mice, labeled with PKH67 cell tracker and injected via tail vein (1×10^6 cells) into WT mice that were fed with CRD alone or in combination with RvD1 or left on CD for 12 weeks and 24 h later the aortas were isolated, cleaned, fixed, opened, mounted on a slide with luminal side up and examined under a Zeiss inverted fluorescent microscope (Axio Observer.Z1). PKH67-positive cells were counted and expressed as cells/field. The values are expressed as Mean ± SD (n = 6). *p < 0.05 vs CD; **p < 0.05 vs CRD. Scale bar, 20 μm.

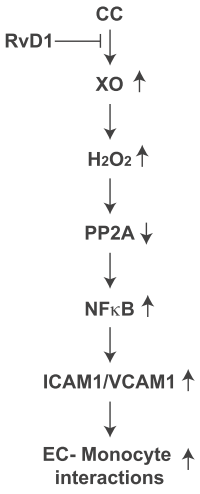

Fig. 8. The schematic diagram depicting the signaling events by which CCs can enhance EC-monocyte interactions and their suppression by RvD1.

Allopurinol, a specific inhibitor of XO [28]. One of the potential mechanisms of H_2O_2 in the mediation of NFκB activation could be due to its capacity to inhibit protein phosphatases such as PP2A. Previous studies have shown that tyrosine phosphorylation of the catalytic subunit of PP2A leads to its inactivation [44]. In this context, we found that cholesterol crystals induce tyrosine phosphorylation of PP2A catalytic subunit C and this correlates with inhibition of its activity. In addition, Allopurinol inhibited cholesterol crystals-induced tyrosine phosphorylation of PP2A catalytic subunit C and its activity. Based on these observations it is most likely that inhibition of PP2A activity is involved in cholesterol crystals-induced phosphorylation of IKKα/β, IκB and NFκB. The kinases IKKα/β upon activation by inflammatory molecules, phosphorylates its substrate IκB leading to its ubiquitination and proteasomal degradation and as a result NFκB is relieved from its inhibitory constraint and becomes activated [25,45]. The role of PP2A in cholesterol crystals-induced NFκB activation can be further confirmed by the findings of RvD1, a specialized proresolving lipid mediator [46,47]. Our results show that RvD1 via suppression of XO-mediated H_2O_2 production prevents tyrosine phosphorylation of PP2A-C(α/β) and inactivation by cholesterol crystals, thus promoting the dephosphorylation and inactivation of NFκB. The observation that RvD1 fails to prevent NFκB activation, ICAM1 and VCAM1 expression and EC-monocyte interactions in the presence of pharmacological PP2A inhibitor further confirms the role of PP2A in the modulation of the effects of cholesterol crystals.

One of the mechanisms by which H_2O_2 mediates cellular signaling is its capacity to oxidize the cysteine residues in the catalytic sites of protein tyrosine phosphatases (PTPs) rendering them inactive, which in turn, promotes the phosphorylation and activation of protein tyrosine kinases (PTKs) [48–51]. Previously, we have shown that LPS via XO-mediated ROS production triggers the oxidation of the catalytic cysteine residue of SHP2 leading to its inactivation [27]. It was reported that H_2O_2 inhibits SHP2 activity via oxidation of its catalytic cysteine residue [48,51,52]. Based on these observations, it is possible that cholesterol crystals could inhibit SHP2 activity which in turn may result in increased PP2A-C(α/β) tyrosine phosphorylation and decreased PP2A activity and thereby leading to NFκB activation. Our in vitro studies on the effects of cholesterol crystals in ECs can be supported by the observations that feeding mice with CRD triggers XO induction, H_2O_2 production, NFκB activation, ICAM1 and VCAM1 expression in the arteries and monocyte recruitment to the arteries in vivo. In addition, RvD1 via preventing XO-mediated H_2O_2 production and PP2A inhibition reversed all the adverse effects of cholesterol crystals on NFκB activation, ICAM1 and VCAM1 expression and monocyte recruitment to the arteries. In conclusion, as depicted in Fig. 8, the present study provides evidence that cholesterol crystals by XO-mediated H_2O_2 production leads to inhibition of PP2A activity, activation of NFkB and expression of ICAM1 and VCAM1 facilitating EC-monocyte interactions, events that play a critical role in atherogenesis. Since the protective effects of RvD1 were linked primarily to its efficacy to suppress cholesterol crystals-induced H_2O_2 production and PP2A inhibition, it is possible that RvD1 acts as an oxidant scavenger.

Conflict of interest

None.

Contributions

PP performed all the experiments and wrote the initial draft of the manuscript; AMM fed animals, assayed PP2A activity, measured H_2O_2 production and performed Western blotting; NKS performed leukocyte trafficking; GNR conceived the overall scope of the project, designed the experiments, interpreted the data and contributed in writing the manuscript.

Acknowledgements

This work was supported by NIH grant HL074860 to GNR.

References

[1] J.R. Vane, E.E. Anggard, R.M. Botting, Regulatory functions of the vascular endothelium, N. Engl. J. Med. 323 (1990) 27–36.
[2] R. Ross, Atherosclerosis: an inflammatory disease, N. Engl. J. Med. 340 (1999) 115–126.
[3] X. Pi, L. Xie, C. Patterson, Emerging roles of vascular endothelium in metabolic homeostasis, Circ. Res. 123 (2018) 477–494.
[4] T. Gerhardt, K. Ley, Monocyte trafficking across the vessel wall, Cardiovasc. Res. 107 (2015) 321–330.
[5] H.B. Shu, A.B. Agranoff, E.G. Nabel, K. Leung, C.S. Duckett, A.S. Neish, T. Collins, G.J. Nabel, Differential regulation of vascular cell adhesion molecule 1 gene expression by specific NF-kappa B subunits in endothelial and epithelial cells, Mol. Cell Biol. 13 (1993) 6283–6289.
[6] J.K. Liao, Linking endothelial dysfunction with endothelial cell activation, J. Clin. Invest. 123 (2013) 540–541.
[7] J.M. Cook-Mills, M.E. Marchese, H. Abdala-Valencia, Vascular cell adhesion molecule-1 expression and signaling during disease: regulation by reactive oxygen species and antioxidants, Antioxidants Redox Signal. 15 (2011) 1607–1638.
[8] K.K. Griendling, G.A. FitzGerald, Oxidative stress and cardiovascular injury: part I: basic mechanisms and in vivo monitoring of ROS, Circulation 108 (2003) 1912–1916.
[9] K.K. Griendling, G.A. FitzGerald, Oxidative stress and cardiovascular injury: part II: animal and human studies, Circulation 108 (2003) 2034–2040.
[10] M.J. Zhang, M. Spite, Resolvins: anti-inflammatory and proresolving mediators derived from omega-3 polyunsaturated fatty acids, Annu. Rev. Nutr. 32 (2012) 203–227.
[11] R. Chattopadhyay, S. Raghavan, G.N. Rao, Resolvin D1 via prevention of ROS-mediated SHP2 inactivation protects endothelial adherens junction integrity and barrier function, Redox Biol. 12 (2017) 438–455.
[12] G.S. Abela, K. Aziz, A. Vedre, D.R. Pathak, J.D. Talbott, J. Dejong, Effect of cholesterol crystals on plaques and intima in arteries of patients with acute coronary and cerebrovascular syndromes, Am. J. Cardiol. 103 (2009) 959–968.
[13] G.S. Abela, J.K. Kalavakunta, A. Janoudi, D. Leffler, G. Dhar, N. Salehi, J. Cohn, I. Shah, M. Karve, V.P.K. Kotaru, V. Gupta, S. David, K.K. Narisetty, M. Rich, A. Vanderberg, D.R. Pathak, F.E. Shamoun, Frequency of cholesterol crystals in culprit coronary artery aspirate during acute myocardial infarction and their relation to inflammation and myocardial injury, Am. J. Cardiol. 120 (2017) 1699–1707.
[14] Y. Kataoka, R. Puri, M. Hammadah, B. Duggal, K. Uno, S.R. Kapadia, E.M. Tuzcu, S.E. Nissen, S.J. Nicholls, Cholesterol crystals associate with coronary plaque vulnerability in vivo, J. Am. Coll. Cardiol. 65 (2015) 630–632.
[15] Z. Chen, M. Ichetovkin, M. Kurtz, E. Zycband, D. Kawka, J. Woods, X. He, A.S. Plump, E. Hailman, Cholesterol in human atherosclerotic plaque is a marker for underlying disease state and plaque vulnerability, Lipids Health Dis. 9 (2010) 61–68.
[16] S. Kotla, N.K. Singh, G.N. Rao, ROS via BTK-p300-STAT1-PPARγ signaling activation mediates cholesterol crystals-induced CD36 expression and foam cell formation, Redox Biol. 11 (2017) 350–364.
[17] A.M. Mani, R. Chattopadhyay, N.K. Singh, G.N. Rao, Cholesterol crystals increase vascular permeability by inactivating SHP2 and disrupting adherens junctions, Free Radic. Biol. Med. 123 (2018) 72–84.
[18] R. Chattopadhyay, E. Dyukova, N.K. Singh, M. Ohba, J.A. Mobley, G.N. Rao, Vascular endothelial tight junctions and barrier function are disrupted by 15(S)-hydroxyeicosatetraenoic acid partly via protein kinase C ε-mediated zona occludens-1 phosphorylation at threonine 770/772, J. Biol. Chem. 289 (2014) 3148–3163.
[19] U. Narayanan, V. Nalavadi, M. Nakamoto, D.C. Pallas, S. Ceman, G.J. Bassell, S.T. Warren, FMRP phosphorylation reveals an immediate-early signaling pathway triggered by group I mGluR and mediated by PP2A, J. Neurosci. 27 (2007) 14349–14357.
[20] V. Kundumani-Sridharan, E. Dyukova, D.E. Hansen 3rd, G.N. Rao, 12/15-Lipoxygenase mediates high fat diet-induced endothelial tight junction disruption and monocyte transmigration: a new role for 15(S)-hydroxyeicosatetraenoic acid in endothelial cell dysfunction, J. Biol. Chem. 288 (2013) 15830–15842.
[21] P. Duewell, H. Kono, K.J. Rayner, C.M. Sirois, G. Vladimer, F.G. Bauernfeind, G.S. Abela, L. Franchi, G. Nunez, M. Schnurr, T. Espevik, E. Lien, K.A. Fitzgerald, K.L. Rock, K.J. Moore, S.D. Wright, V. Hornung, E. Latz, NLRP3 inflammasomes are required for atherogenesis and activated by cholesterol crystals, Nature 464 (2010) 1357–1361.
[22] D.L. Rainwater, Q. Shi, M.C. Mahaney, V. Hodara, J.L. Vandeberg, X.L. Wang, Genetic regulation of endothelial inflammatory responses in baboons, Arterioscler. Thromb. Vasc. Biol. 30 (2010) 1628–1633.
[23] W.A. Muller, G.J. Randolph, Migration of leukocytes across endothelium and beyond: molecules involved in the transmigration and fate of monocytes, J. Leukoc. Biol. 66 (1999) 698–704.
[24] T. Collins, Endothelial nuclear factor-kappa B and the initiation of the atherosclerotic lesion, Lab. Invest. 68 (1993) 499–508.
[25] A. Israel, Signal transduction. I kappa B kinase all zipped up, Nature 388 (1997) 519–521.
[26] P. Karki, J. Johnson Jr., D.S. Son, M. Aschner, E. Lee, Transcriptional regulation of human transforming growth factor-α in astrocytes, Mol. Neurobiol. 54 (2017) 964–976.
[27] R. Chattopadhyay, A.M. Mani, N.K. Singh, G.N. Rao, Resolvin D1 blocks H_2O_2-mediated inhibitory crosstalk between SHP2 and PP2A and suppresses endothelial-monocyte interactions, Free Radic. Biol. Med. 117 (2018) 119–131.
[28] S. Guthikonda, C. Sinkey, T. Barenz, W.G. Haynes, Xanthine oxidase inhibition reverses endothelial dysfunction in heavy smokers, Circulation 107 (2003) 416–421.
[29] M. Kawada, M. Amemiya, M. Ishizuka, T. Takeuchi, Cytostatin, an inhibitor of cell adhesion to extracellular matrix, selectively inhibits protein phosphatase 2A, Biochim. Biophys. Acta 1452 (1999) 209–217.
[30] O. Yoneda, T. Imai, S. Goda, H. Inoue, A. Yamauchi, T. Okazaki, H. Imai, O. Yoshie, E.T. Bloom, N. Domae, H. Umehara, Fractalkine-mediated endothelial cell injury by NK cells, J. Immunol. 164 (2000) 4055–4062.
[31] G.K. Hansson, P. Libby, The immune response in atherosclerosis: a double-edged sword, Nat. Rev. Immunol. 6 (2006) 508–519.
[32] G.K. Hansson, A. Hermansson, The immune system in atherosclerosis, Nat. Immunol. 12 (2011) 204–212.
[33] N. Kume, E. Nishi, K. Tanoue, M. Miyasaka, T. Kita Sakai, P-selectin and vascular cell adhesion molecule-1 are focally expressed in aortas of hypercholesterolemic rabbits before intimal accumulation of macrophages and T lymphocytes, Arterioscler. Thromb. Vasc. Biol. 17 (1997) 310–316.
[34] C.G. Kevil, J.H. Chidlow, D.C. Bullard, D.F. Kucik, High-temporal-resolution analysis demonstrates that ICAM-1 stabilizes WEHI 274.1 monocytic cell rolling on endothelium, Am. J. Physiol. Cell Physiol. 285 (2003) C112–C118.
[35] I. Tabas, K.E. Bornfeldt, Macrophage phenotype and function in different stages of atherosclerosis, Circ. Res. 118 (2016) 653–667.
[36] Y. Baumer, S. McCurdy, T.M. Weatherby, N.N. Mehta, S. Halbherr, P. Halbherr, N. Yamazaki, W.A. Boisvert WA, Hyperlipidemia-induced cholesterol crystal production by endothelial cells promotes atherogenesis, Nat. Commun. 8 (2017) 1129.
[37] S.S. Bakke, M.H. Aune, N. Niyonzima, K. Pilely, L. Ryan, M. Skjelland, P. Garred, P. Aukrust, B. Halvorsen, E. Latz, J.K. Damås, T.E. Mollnes, T. Espevik, Cyclodextrin reduces cholesterol crystal-induced inflammation by modulating complement activation, J. Immunol. 199 (2017) 2910–2920.
[38] K. Brand, S. Page, G. Rogler, A. Bartsch, R. Brandl, R. Knuechel, Activated transcription factor nuclear factor-kappa B is present in the atherosclerotic lesion, J. Clin. Invest. 97 (1996) 1715–1722.
[39] L. Hajra, A.I. Evans, M. Chen, S.J. Hyduk, T. Collins, M.I. Cybulsky, The NF-kappa B signal transduction pathway in aortic endothelial cells is primed for activation in regions predisposed to atherosclerotic lesion formation, Proc. Natl. Acad. Sci. 97 (2000) 9052–9057.
[40] A. Bowie, L.A. O'Neill, Oxidative stress and nuclear factor-kappaB activation: a reassessment of the evidence in the light of recent discoveries, Biochem. Pharmacol. 59 (2000) 13–23.
[41] M.S. Hayden, S. Ghosh, Shared principles in NF-kappaB signaling, Cell 132 (2008) 344–362.
[42] H. Ichikawa, S. Flores, P.R. Kvietys, R.E. Wolf, T. Yoshikawa, D.N. Granger, T.Y. Aw, Molecular mechanisms of anoxia/reoxygenation-induced neutrophil adherence to cultured endothelial cells, Circ. Res. 81 (1997) 922–931.
[43] G.P. Sorescu, H. Song, S.L. Tressel, J. Hwang, S. Dikalov, D.A. Smith, N.L. Boyd, M.O. Platt, B. Lassègue, K.K. Griendling, H. Jo, Bone morphogenic protein 4 produced in endothelial cells by oscillatory shear stress induces monocyte adhesion by stimulating reactive oxygen species production from a Nox1-based NADPH oxidase, Circ. Res. 95 (2004) 773–779.
[44] J. Chen, B.L. Martin, D.L. Brautigan, Regulation of protein serine-threonine phosphatase type-2A by tyrosine phosphorylation, Science 257 (1992) 1261–1264.
[45] A. Israel, The IKK complex, a central regulator of NF-kappaB activation, Cold Spring Harb. Perspect. Biol. 2 (2010) a000158.
[46] M. Spite, J. Clària, C.N. Serhan, Resolvins, specialized proresolving lipid mediators, and their potential roles in metabolic diseases, Cell Metabol. 19 (2014) 21–36.
[47] C.N. Serhan, B.D. Levy, Resolvins in inflammation: emergence of the pro-resolving superfamily of mediators, J. Clin. Invest. 128 (2018) 2657–2669.
[48] T.C. Meng, T. Fukada, N.K. Tonks, Reversible oxidation and inactivation of protein tyrosine phosphatases in vivo, Mol. Cell. 9 (2002) 387–399.
[49] L. Chen, L. Liu, S. Huang, Cadmium activates the mitogen-activated protein kinase (MAPK) pathway via induction of reactive oxygen species and inhibition of protein phosphatases 2A and 5, Free Radic. Biol. Med. 45 (2008) 1035–1044.
[50] J. Oh, M.W. Hur, C.E. Lee, SOCS1 protects protein tyrosine phosphatases by thioredoxin upregulation and attenuates Jaks to suppress ROS-mediated apoptosis, Oncogene 28 (2009) 3145–3156.
[51] R. Karisch, B.G. Neel, Methods to monitor classical protein-tyrosine phosphatase oxidation, FEBS J. 280 (2013) 459–475.
[52] E. Boedtkjer, C. Aalkjaer, Insulin inhibits Na+/H+ exchange in vascular smooth muscle and endothelial cells in situ: involvement of H2O2 and tyrosine phosphatase SHP-2, Am. J. Physiol. Heart Circ. Physiol. 296 (2009) H247–H255.